Eur Biophys J (1992) 21, 337–344

European Biophysics Journal

Interaction of recombinant human epidermal growth factor with phospholipid vesicles. A steady-state and time-resolved fluorescence study of the bis-tryptophan sequence (TRP_{49}-TRP_{50})

Ines M. Li De La Sierra [1], Michel Vincent [2], Gabriel Padron [1], and Jacques Gallay [2]*

[1] Centro de Ingeneria Genetica y Biotecnologia, Apartado postal 6162 Habana, Cuba
[2] Laboratoire pour l'Utilisation du Rayonnement Electromagnétique, Centre National de la Recherche Scientifique, Ministère de l'Education Nationale et de la Jeunesse et des Sports, Commissariat à l'Energie Atomique, Université Paris Sud, Bâtiment 209D-91405 ORSAY Cedex, France,

Received March 29, 1992/Accepted September 18, 1992

Abstract. The interaction of recombinant human epidermal growth factor with small unilamellar phospholipid vesicles was studied by steady-state and time-resolved fluorescence of the bis-tryptophan sequence (Trp_{49}-Trp_{50}). Steady-state anisotropy measurements demonstrate that strong binding occurred with small unilamellar vesicles made up of acidic phospholipids at acidic pH only ($pH \leq 4.7$). An apparent stoichiometry for 1,2-dimyristoyl-*sn*-phosphoglycerol of about 12 phospholipid molecules per molecule of human epidermal growth factor was estimated. The binding appears to be more efficient at temperatures above the gel to liquid-crystalline phase transition. The conformation and the environment of the Trp-Trp sequence are not greatly modified after binding, as judged from the invariance of the excited state lifetime distribution and from that of the fast processes affecting the anisotropy decay. This suggests that the Trp-Trp sequence is not embedded within the bilayer, in contrast to the situation in surfactant micelles (Mayo et al. 1987; Kohda and Inigaki 1992).

Key words: Human recombinant epidermal growth factor – Lipid-protein interactions – Time-resolved fluorescence – Bis-tryptophan

Introduction

Human epidermal growth factor (hEGF)* is a single chain polypeptide of 53 aminoacids (Taylor et al. 1972). It belongs to the large family of proteins which act on cellular development *via* a primary interaction with a membrane-bound receptor located on the cell plasma membrane (Cohen 1962; Carpenter 1987; Yarden and Ullrich 1988; Carpenter and Cohen 1990). According to the "membrane-catalyst" model (Sargent and Schwyzer 1986), this initial process can be divided into a series of substeps. The first molecular events consist of the adsorption of the protein on the membrane surface resulting from electrostatic interactions with phospholipids. This first step can be followed by conformational changes and restriction of the internal dynamics of the peptide. Eventually, insertion of a part of the peptide molecule within the lipid bilayer can take place. Finally, two-dimensional lateral diffusion in the membrane plane and interaction with the receptor occurs. All these steps can contribute to the total free energy of formation of the hormone-receptor complex. Studies of the interactions of hEGF with model membranes can therefore yield information on the possible conformational changes undergone by this protein after binding to cellular membranes. This interaction has been modelled by using surfactant micelles in NMR studies (Mayo et al. 1987; Khoda and Inagaki 1992). Such systems have been chosen in particular because their sizes are relatively small as compared to that of phospholipid vesicles.

The time-resolved fluorescence technique is not sensitive to the slow tumbling of SUV, which is a serious drawback in conventional NMR studies. Information on the conformational and dynamic changes of proteins in these systems, which more closely resemble cell membranes than do surfactant micelles, although the latter have been demonstrated to maintain the enzymatic activities of solubilized membrane-bound enzymes (Tanford and Reynolds 1976), can be obtained from the fluorescence technique (see for instances Vogel et al. 1988; Datema et al. 1987; John and Jähnig 1988; Harnois et al. 1988; Vincent and Gallay 1991). The presence of a Trp-Trp sequence in the hEGF molecule is particularly attractive for fluorescence studies since it can be used as a spectroscopic reporter of environment changes occurring upon interaction with the membrane phospholipids and/or with the soluble part of the receptor (Greenfield et al. 1989). The

* *Correspondence to:* Jacques Gallay, LURE, UPS Bât 209 D, 91 405 Orsay Cedex-France

Abbreviations: DMPG: 1,2-dimyristoyl-*sn*-phosphoglycerol; hEGF: human Epidermal Growth Factor; HPLC: high performance liquid chromatography; MEM: Maximum Entropy Method; POPC: 1-palmitoyl, 2-oleoyl-*sn*-phosphocholine; POPS: 1-palmitoyl, 2-oleoyl-*sn*-phosphoserine; SUV: small unilamellar vesicles; Trp: tryptophan; Trp-Trp: bis-tryptophan

results show that, in contrast to the interaction with surfactant micelles (Mayo et al. 1987; Khoda and Inagaki 1992), hEGF bind efficiently only to negatively charged phospholipids. This binding is strongly dependent on pH and ionic strength.

Materials and methods

Chemicals

Phospholipids (1-palmitoyl-2-oleoyl-*sn*-phosphoserine, 1-palmitoyl-2-oleoyl-*sn*-phosphocholine and 1,2-dimyristoyl-*sn*-phosphoglycerol) were obtained from Avanti Polar Lipids. Beef heart cardiolipin was from Sigma. Their purity was checked by conventional thin layer chromatography.

EGF preparation

hEGF was expressed in *Saccharomyces cerevisiae* and purified by ion exchange chromatography and gel filtration chromatography. After this purification procedure the product contains two EGF species named EGF-1 and EGF-2 differing by one aminoacid but displaying the same biological activity and the same aminoacid sequence except at the C-terminal end (Besada et al. 1990). EGF-2 lacks Arg-53 whereas EGF-1 lacks Leu-52 and Arg-53. EGF species were separated by reverse phase HPLC as described (Besada et al. 1990). In this study, pure EGF-2 was used. The concentration of hEGF was determined spectrophotometrically using an absorption coefficient based on quantitative aminoacid analysis: $E_{0.1\%}=3.1$ at 280 nm.

SUV preparation

Phospholipids were solubilized in chloroform (Merck, spectrograde quality) and evaporated to dryness at the bottom of a glass tube. Hydratation of the samples was performed with the appropriate buffer and the samples were sonicated with a microtip probe sonifier for 3 minutes (half-time duty cycle) at half power.

Fluorescence measurements

Steady-state fluorescence emission and excitation spectra (excitation bandwidth = 2 nm, emission bandwidth = 4 nm) were obtained with a SLM 8000 spectrofluorimeter interfaced to a MacIntosh SE microcomputer. The steady-state anisotropy values were measured with the same instrument in the T format mode with a bandwidth of 1 nm at the excitation side and using Melles-Griot interference filters ($\lambda_{max}=360$ nm, 10 nm bandwidth) for selection of the emission wavelength. Subtraction of blanks was performed when needed as described previously (Vincent et al. 1982).

Fluorescence intensity and anisotropy decays were obtained using the time-correlated single photon counting technique (Yguerabide 1972) from the polarized components $I_{vv}(t)$ and $I_{vh}(t)$ on the experimental set-up installed on the SB_1 window of the synchrotron radiation machine Super-ACO (Anneau de Collision d'Orsay) which has been described elsewhere (Kuipers et al. 1991). The storage ring provides a light pulse with a full width at half maximum (FWHM) of ~500 ps at a frequency of 8.33 MHz for a double bunch mode. The excitation wavelength was set either at 295 or at 300 nm (bandwidth 5 nm unless otherwise stated). The emission wavelength was set at 350 nm (bandwidth 10 nm unless otherwise stated). A Hamamatsu microchannel plate R1564U-06 was utilized. Data for $I_{vv}(t)$ and $I_{vh}(t)$ were stored in separate memories of a plug-in multichannel analyzer card (Canberra) in a DESKPRO 286 E microcomputer (Compaq). Accumulations were stopped when $\sim 10^5$ counts were stored in the peak channel for the fluorescence intensity decay. Time resolution was routinely ~30 ps channel and 1024 channels were used. The instrumental response function was automatically monitored in alternation with the parallel and perpendicular components of the polarized fluorescence decay by measuring the scattering of a glycogen solution. The automatic sampling of the data was driven by the microcomputer.

Analysis of the fluorescence intensity decay and of the fluorescence anisotropy decay

Analysis of the fluorescence intensity decay data by MEM has been described elsewhere (Livesey and Brochon 1987; Vincent et al. 1988; Merola et al. 1989; Gentin et al. 1990; Kuipers et al. 1991). The time-resolved fluorescence anisotropy decay data were analyzed by MEM (Vincent and Gallay 1991). The MEMSYS5 package software (Maximum Entropy Data Consultants Ltd, Cambridge) has been used.

The principles of MEM as applied to time-resolved fluorescence are outlined in the following. With vertically polarized light, the parallel $I_{vv}(t)$ and perpendicular $I_{vh}(t)$ components of the fluorescence intensity at time t after the start of the excitation are:

$$I_{vv}(t) = \tfrac{1}{3} E_\lambda(t) * \int_0^\infty \int_0^\infty \int_{-0.2}^{0.4} \gamma(\tau,\theta,A)\, e^{-t/\tau}(1+2A\, e^{-t/\theta})\, d\tau\, d\theta\, dA \quad (1)$$

and

$$I_{vh}(t) = \tfrac{1}{3} E_\lambda(t) * \int_0^\infty \int_0^\infty \int_{-0.2}^{0.4} \gamma(\tau,\theta,A)\, e^{-t/\tau}(1-A\, e^{-t/\theta})\, d\tau\, d\theta\, dA \quad (2)$$

where $E_\lambda(t)$ is the temporal shape of the excitation flash, * denotes a convolution product and $\gamma(\tau,\theta,A)$ represents the number of fluorophores with fluorescence lifetime τ, rotational correlation time θ and initial anisotropy A.

The total intensity decay parameter, is defined by summing the parallel and perpendicular components:

$$T(t) = I_{vv}(t) + 2I_{vh}(t) = E_\lambda(t) * \int_0^\infty \alpha(\tau) \exp(-t/\tau)\, d\tau \quad (3)$$

$\alpha(\tau)$ is the lifetime distribution given by:

$$\alpha(\tau)=\int_0^{\infty}\int_{-0.2}^{0.4}\gamma(\tau,\theta,A)\,d\theta\,dA \tag{4}$$

In order to ensure our recovered distribution agrees with our data, the Shannon-Jayne entropy S is maximized:

$$S=\int_0^{\infty}\alpha(\tau)-m(\tau)-\alpha(\tau)\log\frac{\alpha(\tau)}{m(\tau)}\,d\tau \tag{5}$$

where $m(\tau)$ is the starting lifetime distribution flat in $\log\tau$ space and $\alpha(\tau)$ is the resulting distribution.

S is subjected to the following constraint:

$$\sum_{k=1}^{M}\frac{(T_k^{calc}-T_k^{obs})^2}{\sigma_k^2}\leq M \tag{6}$$

where T_k^{calc} and T_k^{obs} are the k calculated and observed intensities. σ_k^2 is the variance of the k point ($\sigma_k^2=\sigma_{k,vv}^2+4\beta_{corr}^2\sigma_{k,vh}^2$, Wahl 1979). M is the total number of observations and β_{corr} is a factor compensating for the difference in transmission by the emission monochromator of the parallel and perpendicular light.

The center τ_j of a single class j of lifetimes over the $\alpha(\tau_i)$ distribution is defined as:

$$\tau_j=\sum_i\alpha_i(\tau_i)\,\tau_i/\sum_i\alpha_i(\tau_i) \tag{7}$$

The summation is performed on the significant values of the $\alpha_i(\tau_i)$ for the j class. C_i is the normalized contribution of the lifetimes class j. A lifetime domain spanning 150 values, equally spaced on a logarithmic scale between 0.1 and 20.0 ns, was routinely used in the analyses.

In the analysis of the fluorescence anisotropy decay data all the emitting species are assumed to display the same intrinsic anisotropy and rotational dynamics. In this case, (1) and (2) can be rewritten as:

$$I_{vv}(t)=\tfrac{1}{3}E_\lambda(t)*\int_0^{\infty}\alpha(\tau)\,e^{-t/\tau}\,d\tau\,[1+2\int_0^{\infty}\beta(\theta)\,e^{-t/\theta}\,d\theta] \tag{8}$$

and

$$I_{vh}(t)=\tfrac{1}{3}E_\lambda(t)*\int_0^{\infty}\alpha(\tau)\,e^{-t/\tau}\,d\tau\,[1-\int_0^{\infty}\beta(\theta)\,e^{-t/\theta}\,d\theta] \tag{9}$$

with

$$A_0=\int_0^{\infty}\beta(\theta)\,d\theta\,, \tag{10}$$

where $\beta(\theta)$ is the rotational correlation time distribution and the other symbols have the same significance as in (1). The $\alpha(\tau)$ profile is given from a first analysis of $T(t)$ by MEM and is held constant in a subsequent and global analysis of $I_{vv}(t)$ and $I_{vh}(t)$ which provides the distribution $\beta(\theta)$ of correlation times. 100 rotational correlation time values, equally spaced in logarithmic scale and ranging from 0.01 to 20 ns were used for the analysis of $\beta(\theta)$.

The barycenters for the correlation time distribution are calculated as:

$$\theta_j=\frac{\sum_i\beta_i(\theta_i)\,\theta_i}{\sum_i\beta_i(\theta_i)} \tag{11}$$

β_i is the contribution of the rotational correlation time i to the class j.

Binding of hEGF to SUV

This binding was monitored by measuring the steady-state anisotropy value of the Trp emission as a function of SUV addition. According to the simplest formulation of Perrin's law for rigid sphere (Perrin 1926):

$$(r_0/r_s)-1=\langle\tau\rangle/\theta \tag{12}$$

where r_s is the steady-state anisotropy measured at the absolute temperature T and viscosity η, r_0 is the intrinsic anisotropy measured in the absence of Brownian rotational motion and energy transfer, $\langle\tau\rangle$ is the average excited state lifetime of the fluorophore and θ is the rotational correlation time. According to the Stockes-Einstein relation, the rotational correlation time describing the brownian motion is proportional to the hydrated volume V_h of the particle, to the viscosity and to the reciprocal of the temperature:

$$\theta=(V_h\,\eta)/kT \tag{13}$$

When the protein is bound to SUV, the volume of the rotating particle increases tremendously and the measured steady-state anisotropy value is increased. This variation provides a sensitive test of protein binding since the lifetime variations are much less important than those of the rotational correlation times.

Results

Steady-state anisotropy measurements

The steady-state anisotropy of the Trp emission of hEGF in solution at pH 3.6 and 20 °C is slightly increased after stepwise addition of POPC SUV, indicating that the

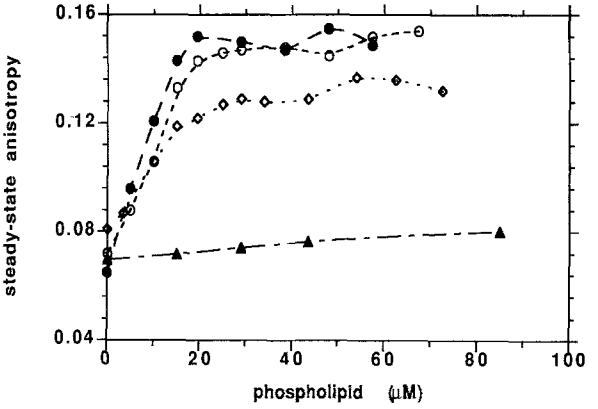

Fig. 1. Variation of the steady-state anisotropy of Trp-Trp emission in hEGF as a function of phospholipid concentration at pH 3.6 (▲) POPC SUV at 20 °C; (◇) DMPG SUV at 10 °C; (○) DMPG SUV at 20 °C and (●) DMPG SUV at 37 °C. Excitation wavelength: 300 nm (2 nm bandwidth), emission wavelength: 360 nm. hEGF concentration: 1.6 μM

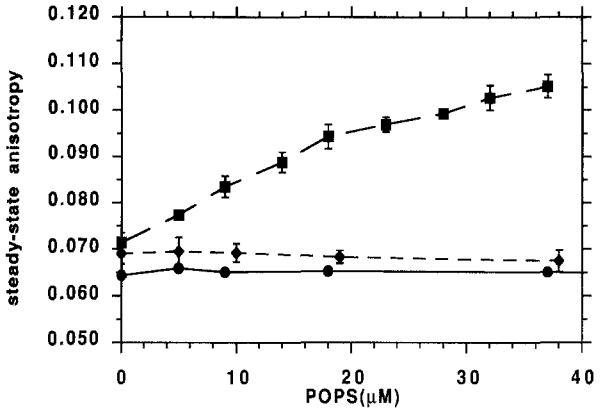

Fig. 2. Variation of the steady-state anisotropy of Trp-Trp emission in hEGF as a function of POPS-SUV concentration at 20 °C. (■) pH 8; (♦) pH 5.6 and (●) pH 3.6. Same experimental conditions as in Fig. 1

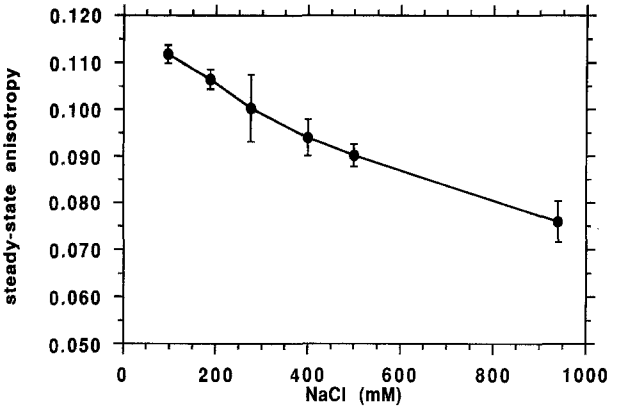

Fig. 3. Variation of the steady-state anisotropy of Trp-Trp emission in hEGF in the presence of POPS-SUV as a function of the ionic strength at pH 3.6. Same experimental conditions as in Fig. 1

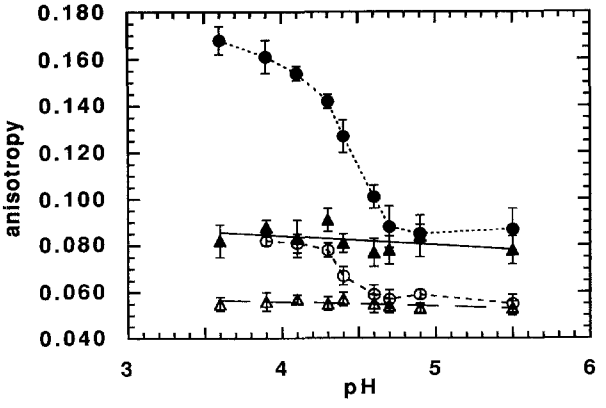

Fig. 4. Effect of pH on the association of hEGF with DMPG SUV at 20 °C as monitored by steady-state anisotropy measurements. The filled symbols (●, ▲) correspond to excitation wavelength of 300 nm, the empty symbols (○, △) correspond to excitation wavelength of 295 nm. As a control, the variation of the steady-state anisotropy of hEGF in solution was also measured at both excitation wavelengths: 295 nm (△) and 300 nm (▲). Emission wavelength: 360 nm (Melles Griot interference filter, 10 nm bandwidth). hEGF concentration: 1.6 μM. Temperature 20 °C

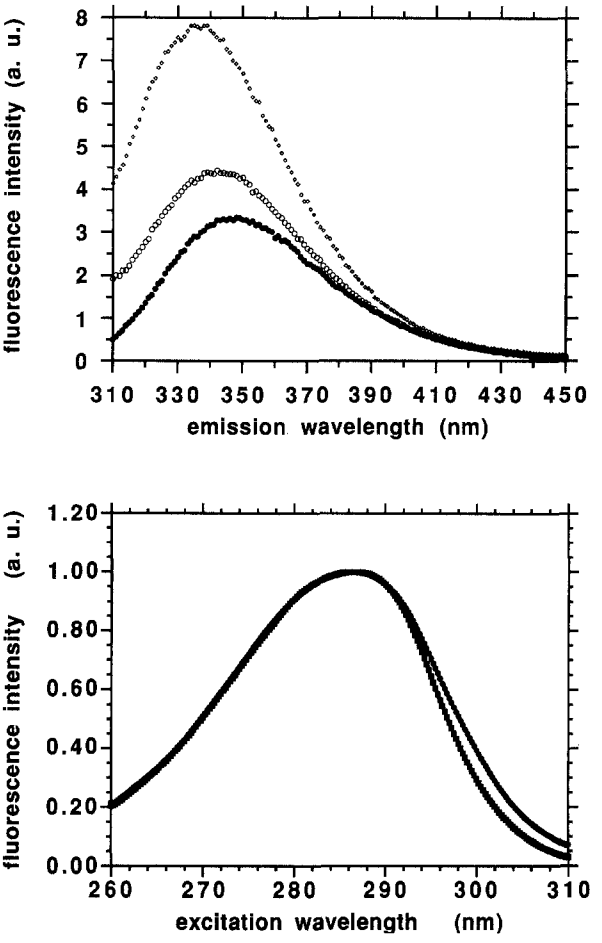

Fig. 5. Fluorescence excitation and mission spectra of hEGF associated with negatively charged phospholipid SUV. *Upper panel*: fluorescence emission spectra of hEGF in acetate buffer pH 3.6 (●); fluorescence emission spectra of hEGF in acetate buffer pH 3.6 associated with DMPG SUV (lipid/protein mole ratio = 20) (○); fluorescence emission spectra of hEGF in acetate buffer pH 3.6 associated with cardiolipin SUV (lipid/protein mole ratio ~100) (◇). Excitation wavelength: 295 nm (4 nm bandwidth). Temperature 20 °C. *Lower panel*: fluorescence excitation spectra of hEGF in acetate buffer pH 3.6 (■) and associated to DMPG SUV (○) nm. Emission wavelength: 360 nm. Protein concentration 1.6 μM

protein undergoes some interactions with this neutral phospholipid (Fig. 1). A much larger increase is observed in the case of DMPG SUV addition (Fig. 1). The temperature of the gel-to-liquid phase transition of DMPG is known to be dependent on pH (Van Dijck et al. 1978). At pH 3.6, this critical temperature value is around 30 °C. The interaction of hEGF with DMPG was studied at different temperatures in order to test whether it depended on the lipid phase organization or not. It can be seen from the data presented in Fig. 1 that the increase in the steady-state anisotropy value is steeper at 37 °C than at 10 °C and that the plateau value is also higher. From the intersection of the rising part of the curve and of the plateau value, an approximate stoichiometric ratio of about 12 DMPG molecules for one hEGF molecule can be estimated for minimal binding.

The nature of the driving forces stabilizing the interaction of hEGF with phospholipid vesicles was investigated

by changing the pH. It can be seen that binding to POPS SUV, for instance, is dramatically dependent on pH (Fig. 2). Binding can only be observed at acidic pH, no significant binding occurs at pH 5.6 or 8. The reversibility of the interaction was checked by increasing the ionic strength and pH in the case of preformed hEGF-SUV-POPS complexes. The steady-state anisotropy value decreased to that observed in the absence of SUV, indicating therefore that no aggregation of the hEGF molecule is occurring as a function of the salt concentration (Fig. 3).

To test further the pH effect, DMPG-SUV were prepared in buffer at different pH and were added to hEGF in saturating conditions obtained at pH 3.6. The curve of the titration experiment shows that the interaction disappears above pH 4.7 (Fig. 4). A pK of about 4.4 can be estimated. As a control, the steady-state value of hEGF as a function of pH was measured (Fig. 3) without any evidence for a variation.

Steady-state excitation and emission spectra

The binding of hEGF to SUV made up of negatively charged phospholipids modified the excitation and emission spectra (Fig. 5). A blue-shift of about 5 nm and a slight increase in fluorescence intensity are observed after binding to DMPG SUV at low lipid/protein ratio (Ri). The effect is stronger in cardiolipin vesicles. The excitation spectrum shows a significant increase in intensity only in the 300 nm region, probably revealing a similar modification in the absorption spectrum which cannot be recorded owing to the large perturbation by scattered light (Fig. 5).

Time-resolved fluorescence measurements

Excited state lifetime measurements show only slight change in the lifetime profile, as obtained by MEM, in the complex with DMPG as compared to hEGF in buffer pH 3.6, whatever the temperature (Table 1). Three major lifetime classes are observed for hEGF in solution. The minor long one is more obvious in the vesicles. A large scatter in this long lifetime value is observed owing to its low contribution. Interaction with cardiolipin leads to similar small effects (Table 1).

The fluorescence anisotropy decay of hEGF in buffer solution is described by 3 time components at low temperatures (Table 2). The longest component is due to the overall Brownian motion of the protein and its value (3.5 ns) most likely corresponds to a monomer at this concentration of protein (1.6 μM). The shortest most likely corresponds to fast rotational motion of the indole ring and to twisting motions of the C-terminal peptide segment as recent results with single Trp mutants indicate

Table 1. Excited state lifetime distribution of Trp49-Trp50 in hEGF in solution pH 3.6 and in interaction with negatively charged phospholipid SUV. Excitation wavelength: 295 nm; emission wavelength: 350 nm. Protein concentration: 1.6 μM. Phospholipid/protein ratio ~20

Experimental conditions	c_1	c_2	c_3	c_4	$\tau_{1(ns)}$	$\tau_{2(ns)}$	$\tau_{3(ns)}$	$\tau_{4(ns)}$	χ^2
10 °C in buffer	0.35	0.30	0.34	–	0.32	1.39	3.49	–	1.05
10 °C + DMPG-SUV	0.43	0.30	0.24	0.02	0.32	1.36	3.34	7.6	1.10
20 °C (*)	0.36 ± 0.01	0.31 ± 0.07	0.33 ± 0.06	0.01 ± 0.01	0.42 ± 0.04	1.57 ± 0.18	3.07 ± 0.19	7.1 ± 1.1	–
20 °C + DMPG-SUV (*)	0.31 ± 0.01	0.32 ± 0.02	0.35 ± 0.01	0.03 ± 0.01	0.38 ± 0.08	1.19 ± 0.06	2.81 ± 0.27	6.6 ± 1.0	–
20 °C + cardiolipin SUV	0.28	0.37	0.33	0.02	0.54	1.55	3.43	9.2	1.03
37 °C	0.32	0.44	0.24	–	0.37	1.34	2.47	–	1.08
37 °C + DMPG SUV	0.25	0.32	0.39	0.03	0.45	1.34	2.47	5.0	1.06

(*) average of 3 experiments

Table 2. Fluorescence anisotropy decay of Trp49-Trp50 in hEGF in solution pH 3.6 associated with phospholipid SUV. Conditions are the same as in Table 1.

Experimental conditions	β_1	β_2	β_3	$\theta_{1(ns)}$	$\theta_{2(ns)}$	$\theta_{3(ns)}$	A_0	χ^2
5 °C in buffer	0.052	0.031	0.109	0.3	1.8	6.5	0.192	1.03
+ DMPG-SUV	0.117	0.026	0.073	0.1	1.6	∞	0.216	1.00
10 °C in buffer	0.048	0.062	0.070	0.2	2.1	6.7	0.189	1.01
+ DMPG-SUV	–	0.030	0.089	–	2.5	∞	0.119	1.07
20 °C in buffer (*)	0.142 ± 0.063	0.046 ± 0.013	0.096 ± 0.006	0.1 ± 0.05	0.7 ± 0.2	3.5 ± 0.3	0.284	–
+ DMPG-SUV	0.074	0.047	0.089	0.1	2.1	∞	0.210	1.00
+ cardiolipin	–	0.014	0.098	–	1.1	32	0.122	1.11
37 °C in buffer	–	0.128	0.111	–	0.2	2.8	0.239	1.07
+ DMPG-SUV	–	0.023	0.097	–	0.6	60	0.120	1.02

(*) average of 3 experiments

(unpublished results). At higher temperature, only two correlation times are detectable (Table 2). The two shortest are too fast at this temperature to be separated. It should be remarked that the A_0 value is close to that expected for the excitation wavelength of 295 nm. No other depolarization motions are present and the anisotropy decay data at short times are described by only one single subnanosecond correlation time.

The major effect of binding of the protein to DMPG-SUV is to increase to extremely long values the rotational correlation time of the peptide, which is a direct proof of a strong binding in these experimental conditions of temperature and pH. This is observed either in the gel or in the fluid lipid phases. Owing to the time window defined by the excited state lifetime distribution, the long correlation times of 32 and 60 ns are not significantly different from an infinite value (Table 2).

The enhancement of the light scattering of the sample due to the increase in the vesicle size or to aggregation following the binding of the protein is a serious drawback for the analysis of the anisotropy at short times. In fact an extremely short time component (a few picoseconds) is always observed in the analysis. This is without any physical meaning since it displays a pre-exponential term higher than 0.4 (not shown). This explains the drop in the A_0 value in the presence of lipid vesicles in some cases. However, when it is possible to separate this scattering contribution, for instance at lower temperature where the fluorescence intensity is higher and the aggregation of the vesicles is apparently less, from the short correlation times, their contributions to the anisotropy are not drastically altered. The increase of the contribution of the short time constant at 5 °C in DMPG is likely to be due to the contribution of light scattering. Since energy homotransfer can occur between the two Trp residues, it is not straightforward at the present stage of the investigation to ascribe these components to rotational dynamics or to energy transfer rates since they will appear on the anisotropy decay as exponential terms (Bastiaens et al. 1989). In some favourable cases, it is possible to take advantage of the red-edge effect (Weber and Shinitzki 1972) to reduce the energy transfer contribution. However, a complete study on the energy transfer mechanism in this molecule and in Trp-Trp is under current investigation using single Trp mutants. Whatever the mechanism may be, the small change of the time components indicates that neither the conformation nor the dynamics of the Trp-Trp sequence are modified upon binding to the membrane.

Discussion

Former studies of the interaction of EGF with membranes using NMR techniques have emphasized that the protein molecule can be readily incorporated into SDS surfactant micelles (Mayo et al. 1987) or dodecylphosphocholine micelles (Khoda and Inagaki 1992), even at neutral pH. As a consequence of this interaction, conformational changes of the C-terminal part of the protein were demonstrated. These studies have indicated that the Trp-Trp sequence was likely to become shielded from interactions with the surrounding water as were Tyr 10 and 37. The most recent study (Khoda and Inagaki 1992) concluded that the C-terminal tail of EGF took on an amphiphilic structure when bound to dodecylphosphocholine micelles.

In the present work, it is unambiguously demonstrated that the interaction of hEGF with a phospholipidic membrane is more critical in terms of specificity of interaction than with micelles. Neutral phospholipids such as POPC, presenting the same zwitterionic polar group as dodecyl phosphocholine, are extremely poor ligands at neutral or acidic pH as compared to negatively charged phospholipids at acidic pH. The negative charge of the phospholipid is not the only prerequisite for the interaction to take place, the overall electrostatic charge of the protein must also be positive, that is the pH must be below the isoelectric point of the protein (pI = 4.6) (Taylor et al. 1972). The repulsion between the negatively charged interface of the acidic phospholipid vesicles and the acidic side chains located for the most part in the N-terminal half of the hEGF molecule is probably the most important contribution to the absence of binding above pH 4.7. In acidic pH conditions, the electrostatic interactions between the basic aminoacid side-chains and the membrane surface are more efficient. The protein region involved in these interactions is probably the C-terminal region. Lys-28, Arg-41, Arg-45 and Lys-48 can constitute such a "binding region". However, the fluorescence parameters of the Trp emission are not dramatically modified after interaction. The small changes in the excited state population distribution of the Trp-Trp sequence after binding to the membranes preclude the possibility of a strong perturbation of its environment, as would have resulted if it was embedded in the membrane bilayer in hydrophobic contacts with fatty acid chains. Even the relative proportions of the excited state lifetime populations are not changed. Therefore the conformation of that peptide segment is not affected by the binding. The absence of hydrophobic interaction of the hEGF molecule with the phospholipids is confirmed by the readily desorption of the protein from the membrane induced by increasing the pH or the ionic strength. It is therefore likely that the Trp-Trp sequence preserves a similar conformation as in the protein free in solution. Interactions of that sequence with the solvent and/or with adjacent peptide groups in the protein are similar at the membrane surface and in solution. The blue shift of the fluorescence emission maximum and the change in the excitation spectrum suggest perturbations of hydrogen bonding (Strickland et al. 1972), most likely due to the more organized hydration water present at the membrane interface.

Therefore, interaction of hEGF with SUV leads to a different type of situation as compared to micellar systems. In these last species, the packing forces at the polar group level are much less than between the phospholipid molecules organized as bilayers. The network of hydrogen bonding between the head groups, especially at low pH, may limit the ability of a rigid molecule such as hEGF (Holladay et al. 1976) to penetrate deeply into the membrane bilayer. EGF, except for its C-terminal part

where the two Trp residues are located, is a rigid undeformable molecule. The molecule is stabilized by a set of three disulfide bonds which define a rigid core structure consisting of three loops and an antiparallel β-sheet comprising Val-19 to Glu-24 and Asp-27 to Asn-32, as shown by ^{1}H-NMR spectroscopy (Makino et al. 1987; Montelione et al. 1992; Cooke et al. 1987; Moy et al. 1989; Mayo et al. 1989). It is therefore likely that it cannot easily undergo adaptative conformational changes in order to be readily accomodated in highly organized molecular assemblies such as these membrane vesicles, even at temperatures above the gel-to-liquid crystalline phase transition. Micellar aggregates are more dynamic and flexible and can accomodate such a strongly structured molecule.

In conclusion, the binding of hEGF to membrane phospholipids occurs primarily *via* electrostatic interactions, in contrast to its binding to micellar systems. These data do not support a penetration of the Trp-Trp sequence into the acyl chain region of the bilayer. The micellar systems may be considered as extremely dynamic assemblies of lipids capable of accomodating such a structured molecule.

Acknowledgements. The authors wish to thank the CNRS (France)-CECE (Cuba) exchange program and INSERM CRE 910915 for partially supporting this work. The technical staff of LURE are acknowledged for running the synchrotron machine during the beam sessions.

References

Bastiaens PH, Bonants PJM, Müller F, Visser AJWG (1989) Time-resolved fluorescence spectroscopy of NADPH-cytochrome P-450 reductase: demonstration of energy transfer between the two prosthetic groups. Biochemistry 28:8416–8425

Besada V, Antuch W, Cinza A, Rojas I, Quintana M, Padrón G (1990) Chemical characterization of recombinant human epidermal growth factor. Anal Chim Acta 235:301–305

Carpenter G (1987) Receptors for epidermal growth factor and other polypeptide mitogens. Ann Rev Biochem 56:881–914

Carpenter G, Cohen S (1990) Epidermal growth factor. J Biol Chem 265:7709–7712

Cohen S (1962) Isolation of a mouse submaxillary protein accelerating incisor eruption and eyelid opening in the new-born animals. J Biol Chem 237:1555–1562

Cooke RM, Wilkinson AJ, Baron M, Pastore A, Tappin MJ, Campbell ID, Gregory H, Sheard B (1987) The solution structure of human epidermal growth structure. Nature 327:339–341

Datema KP, Visser AJWG, van Hoek A, Wolfs CJAM, Spruijt RB, Hemminga MA (1987) Time-resolved tryptophan fluorescence anisotropy investigation of bacteriophage M13 coat protein in micelles and in mixed bilayers. Biochemistry 26:6145–6152

Gentin M, Vincent M, Brochon JC, Livesey AK, Cittanova N, Gallay J (1990) Time-resolved fluorescence of the single tryptophan residue in rat α-fetoprotein and rat serum albumin: analysis by the maximum entropy method. Biochemistry 29:10405–10412

Greenfield C, Hiles I, Waterfield MD, Federwisch M, Wollmer A, Blundell TL, McDonald N (1989) Epidermal growth factor binding induces a conformational change in the external domain of its receptor. EMBO J 8:4115–4123

Harnois I, Genest D, Brochon JC (1988) Micellization and interactions with phospholipid vesicles of the lipopeptide Iturin A, as monitored by time-resolved fluorescence of a D-tyrosyl residue. Biopolymers 27:1403–1413

Holladay LA, Savage CR, Cohen S, Puett D (1976) Conformation and unfolding thermodynamics of epidermal growth factor and derivatives. Biochemistry 15:2624–2633

John E, Jähnig F (1988) Dynamics of melittin in water and membrane as determined by fluorescence anisotropy decay. Biophys J 54:817–827

Kohda D, Inagaki F (1992) Structure of epidermal growth factor bound to perdeuterated dodecylphosphocholine micelles determined by two-dimensional NMR and simulated annealing calculations. Biochemistry 31:677–685

Kuipers OP, Vincent M, Brochon JC, Verheij HM, de Haas GH, Gallay J (1991) Insight into the conformational dynamics os specific regions of porcine pancreatic phospholipase A_2 from a time-resolved fluorescence study of a genetically inserted single tryptophan residue. Biochemistry 30:8771–8785

Livesey AK, Brochon JC (1987) Analyzing the distribution of decay constants in pulse-fluorimetry using the Maximum Entropy Method Biophys J 52:693–706

Makino K, Morimoto M, Nishi M, Sakamoto S, Tamura A, Inooka H, Asaka K (1987) Proton nuclear magnetic resonance study on the solution conformation of human epidermal growth factor. Proc Natl Acad Sci USA 84, 7841–7845

Mayo KH, De Marco A, Menegatti E, Kaptein R (1987) Interaction of epidermal growth factor with micelles monitored by photochemically induced dynamic nuclear polarization-1H NMR spectroscopy. J Biol Chem 262:14899–14904

Mayo KH, Cavalli RC, Peters AR, Boelens R, Kaptein R (1989) Sequence specific ^{1}H-NMR assignments and peptide backbone conformation in rat epidermal growth factor. Biochem J 257:197–205

Merola F, Rigler R, Holmgren A, Brochon JC (1989) Picosecond tryptophan fluorescence of thioredoxin: evidence for discrete species in slow exchange. Biochemistry 28:3383–3398

Montelione GT, Wüthrich K, Burgess AW, Nice EC, Wagner G, Gibson KD, Scheraga HA (1992) Solution structure of epidermal growth factor determined by NMR spectroscopy and refined energy minimization with restraints. Biochemistry 31:236–249

Moy FJ, Scheraga HA, Liu J-F, Wu R, Montelione GT (1989) Conformational characterization of a single-site mutant of murine epidermal growth factor (EGF) by ^{1}H NMR provides evidence that leucine-47 is involved in the interactions with the EGF receptor. Proc Natl Acad Sci USA 86:9836–9840

Perrin F (1926) Polarisation de la lumière de fluorescence. Vie moyenne des molécules dans l'état excité. J de Physique 7:390–401

Sargent DF, Schwyzer R (1986) Membrane lipid phase as catalyst for peptide-receptor interactions. Proc Natl Acad Sci USA 83:5774–5778

Strickland EH, Billups C, Kay E (1972) Effects of hydrogen bonding and solvents upon the tryptophanyl ^1L_a absorption band. Studies using 2,3-dimethylindole. Biochemistry 19:3657–3662

Tanford C, Reynolds JA (1976) Characterization of membrane proteins in detergent solutions. Biochim Biophys Acta 457:133–170

Taylor JM, Mitchell WM, Cohen S (1972) Epidermal growth factor, physical properties. J Biol Chem 247:5928–5934

van Dijck PWM, de Kruijff B, Verkleij AJ, van Deenen LLM, de Gier J (1978) Comparative study on the effects of pH and Ca^{2+} on bilayers of various negatively charged phospholipids and their mixture with phosphatidylcholine. Biochim Biophys Acta 512:84–96

Vincent M, de Foresta B, Gallay J, Alfsen A (1982) Nanosecond fluorescence anisotropy decay of n-(9-anthroyloxy) fatty acids in dipalmitoyl phosphatidylcholine vesicles with regards to isotropic solvents. Biochemistry 21:708–716

Vincent M, Brochon JC, Merola F, Jordi W, Gallay J (1988) Nanosecond dynamics of horse heart apocytochrome *c* in aqueous solution as studied by time-resolved fluorescence of the single tryptophan residue (Trp-59). Biochemistry 27:8752–8761

Vincent M, Gallay J (1991) The interactions of horse heart apocytochrome *c* with phospholipid vesicles and surfactant micelles: time-resolved fluorescence study of the single tryptophan residue (Trp-59). Eur Biophys J 20:183–191

Vogel H, Nilsson L, Rigler R, Voges KP, Jung G (1988) Structural fluctuations of a helical polypeptides traversing a lipid bilayer. Proc Natl Acad Sci USA 85:5067–5071

Wahl PH (1979) Analysis of fluorescence anisotropy decay by least square method. Biophys Chem 10:91–104

Weber G, Shinitzki M (1972) Failure of energy transfer between identical aromatic molecules on excitation at the long wave edge of the absorption spectrum. Proc Natl Acad Sci USA 65:8723–8730

Yarden Y, Ullrich A (1988) Growth factors receptor tyrosine kinases. Ann Rev Biochem 57:443–478

Yguerabide J (1972) Nanosecond spectroscopy of macromolecules. Methods in Enzymology 26 part C:498–578